Available online at www.sciencedirect.com
SCIENCE DIRECT
Journal of Solid State Chemistry 179 (2006) 2093–2100
JOURNAL OF SOLID STATE CHEMISTRY
www.elsevier.com/locate/jssc

Synthesis and characterization of one- to three-dimensional compounds composed of paradodecatungstate-B cluster and transition metals as linkers

Chun-Yan Sun[a], Shu-Xia Liu[a,*], Lin-Hua Xie[a], Chun-Ling Wang[a], Bo Gao[a], Chun-Dan Zhang[a], Zhong-Min Su[b]

[a]*Key Laboratory of Polyoxometalates Science of Ministry of Education, College of Chemistry, Northeast Normal University, Changchun 130024, PR China*
[b]*Faculty of Chemistry, Institute of Functional Materials, Northeast Normal University, Changchun 130024, PR China*

Received 2 January 2006; received in revised form 27 February 2006; accepted 23 March 2006
Available online 15 May 2006

Abstract

Three new extended frameworks built from paratungstate and transition metals have been synthesized and characterized. In the compound $Na_8[\{Cd(H_2O)_2\}(H_2W_{12}O_{42})]\cdot 32H_2O$ (**1**), two neighboring paratungstate-B ions $[H_2W_{12}O_{42}]^{10-}$ are linked by $[Cd(H_2O)_2]^{2+}$ units, leading to the formation of infinite one-dimensional (1D) anion chain $[\{Cd(H_2O)_2\}(H_2W_{12}O_{42})]_n^{8n-}$. The anion $[\{Co(H_2O)_3\}\{Co(H_2O)_4\}(H_2W_{12}O_{42})]_n^{6n-}$ of the compound $Na_6[\{Co(H_2O)_3\}\{Co(H_2O)_4\}(H_2W_{12}O_{42})]\cdot 29H_2O$ (**2**) shows a layer-like (2D) structure in which paratungstate-B units are linked by CoO_6 octahedra, while the anion $[\{Co(H_2O)_3\}_3(H_2W_{12}O_{42})]_n^{4n-}$ of the compound $(H_3O^+)_3[\{Na(H_2O)_4\}\{Co(H_2O)_4\}_3(H_2W_{12}O_{42})]\cdot 24.5H_2O$ (**3**) is a three-dimensional (3D) anionic polymer that consists of paratungstate-B units linked by CoO_6 octahedra. Compound **3** can reversibly adsorb and desorb water molecules leading to the color reversibly change from pink to violet. The preliminary magnetic measurement and electrochemical properties of compounds are performed. The crystal structure of unexpected product $Na_4[NiW_6O_{24}H_6]\cdot 13H_2O$ (**4**) is described here for the rare report of crystal structure information on the Anderson-type polyoxotungstate which has nickel as a heteroatom.

Keywords: Polyoxometalates; Paradodecatungstate; Transition metal; Extend framework; Crystal structure

1. Introduction

Polyoxometalates (POMs) have been a center of research interest for a long time, as they exhibit a great variety of structures and rich diversity of remarkable properties [1]. It is especially fascinating when chemically robust POM clusters are employed as building blocks to construct extended solid frameworks in appropriate ways not only because of the structural and topological novelty of such engineered solids but also due to the potentially interesting electronic, optical, magnetic, catalytic and other properties [2–5]. One of the challenging tasks in POMs chemistry is to link up discrete polyanion units into one-, two- and even three-dimensional (1-, 2- and 3D) extended solid frameworks with desired properties. And it has been shown recently that many inorganic–organic hybrid materials with extended frameworks based on POMs can be obtained, in hydrothermal conditions especially [6]. But bringing suitable metal oxide building blocks together by simple linking units to generate true metal oxide surfaces and framework materials without the incorporation of additional conventional ligands still remains largely to be explored [7]. This kind of material is usually stable and insoluble in common organic solvent, whose property is very advantageous to expand application of POM-based materials in chemically bulk-modified electrode [8]. It is known that transition metal ions exhibit unique catalytic and magnetic properties, which have wide potential applications in material science. With the aim of producing

*Corresponding author. Fax: +86 431 5684009.
E-mail address: liusx@nenu.edu.cn (S.-X. Liu).

0022-4596/$ - see front matter © 2006 Elsevier Inc. All rights reserved.
doi:10.1016/j.jssc.2006.03.048

extended structure, much attention has been focused on developing transition metal-incorporated POMs, in which the transition metal ions are used as linkers. Because of their multiple coordination requirements and oxophilicity, transition metal cations are suitable for linking POM units together to form new classes of materials with extended frameworks.

The linking rules of selected building blocks should also be taken into account. Among the various structures of POMs, one of the most interesting is the paradodecatungstate anion $[H_2W_{12}O_{42}]^{10-}$, which has some particular structural features, and provides a variety of possibilities of intermolecular linkages [1a,9–11]. In this context, we are involved in the synthesis of paradodecatungstate linked by first-row transition metal cations and obtain a series of unique compounds ranging from 1D polymer to 3D architecture in a facile synthetic method, and their interesting properties also reported here.

2. Experimental section

2.1. General procedures

All reagents were of high-purity grade and were used as purchased commercially. Elemental analyses (Co, Cd, Ni, Na, W) were determined by a Leaman inductively coupled plasma (ICP) spectrometer. TG analyses were performed on a Perkin-Elmer TGA7 instrument in flowing N_2 with a heating rate of $10\,^{\circ}C\,min^{-1}$. X-ray powder diffraction (XRPD) experiments were performed in the scattering angle range $2\theta = 3.025-89.975^{\circ}$ with 0.05° steps on a commercial D/max-γA rotating anode X-ray diffractometer using Cu$K\alpha$ radiation of a wavelength $\lambda = 1.54$ Å. The weight loss for a sample heated by a high vacuum oven is measured by an AB104-N photoelectric analytical balance. The magnetic properties of **3** have been performed on a crystalline sample using a Quantum Design MPMS-5 SQUID magnetometer in the range of 2–300 K. Diamagnetic corrections were estimated from Pascal's constants. Cyclic voltammetry measurements were carried out on a CHI 660 electrochemical workstation using a conventional three-electrode single compartment cell at room temperature. The working electrode was a glassy carbon disc electrode or **3**-CPE (carbon paste electrode). The surface of the glass carbon electrode was polished with 0.3 μm alumina and washed with distilled water before each experiment. Platinum gauze was used as counter electrode and an Ag/AgCl was used as reference electrode. The solutions were degassed with pure nitrogen for 15 min before use and blanketed with nitrogen gas during the voltammetric scans. Controlled potential electrolysis experiments were performed using an AUTOLAB PGSTAT 30 potentiostat. The reference electrode was the same as above. A carbon cloth or a platinum mesh was used as the working electrode. The counter electrode was a platinum mesh of large surface area. Experiments were performed at room temperature.

2.2. Synthesis of compounds

Synthesis of 1: $Na_2WO_4 \cdot 2H_2O$ (3.3 g, 10 mmol) was dissolved in 30 mL of water, the solution was heated to 80 °C, 0.1 g boric acid solid was added and the pH of mixture was adjusted to 7 by HCl, and then a solution of $CdCl_2 \cdot 2.5H_2O$ (0.46 g, 2 mmol) in water (2 mL) was added dropwise. If a light turbidity occurred it was waited until it cleared again before the next drop was added. The final pH was adjusted to 6 by addition of diluted HCl. Keep at this temperature for half an hour. The solution was removed from the heat and cooled to room temperature. During a few days, colourless single crystals crystallized out of the solution in the form of perfectly developed parallepipeds. The yield was 45% (based on Cd). Anal. Calcd. (Found) for $Na_8[\{Cd(H_2O)_2\}(H_2W_{12}O_{42})] \cdot 32H_2O$: Na 4.86 (4.89); W 58.20 (58.10); Cd 2.97 (2.93)%. IR (KBr pellet, cm^{-1}): 3470(vs), 1629(s), 952(s), 863(m), 698(m), 423(w).

Synthesis of 2: $Na_{10}[H_2W_{12}O_{42}] \cdot 20H_2O$ (3.6 g, 1 mmol), which was prepared according to Ref. [12], was added to an aqueous solution of CH_3OONa/CH_3COOH buffer (pH 6) (30 mL), heated to 80 °C, and then $CoCl_2 \cdot 6H_2O$ (0.48 g, 2 mmol) was added. The resulting green mixture was stirred for half an hour, cooled to room temperature, and then filtered. During a few days, pink crystals crystallized out of the solution. The yield was 24% (based on Co). Anal. Calcd. (Found) for $Na_6[\{Co(H_2O)_3\}\{Co(H_2O)_4\}(H_2W_{12}O_{42})] \cdot 29H_2O$: Na 3.65 (3.62); W 58.31 (58.29); Co 3.11 (3.17)%. IR (KBr pellet, cm^{-1}): 3400(vs), 1637(s), 925(s), 857(m), 691(m), 522(w), 493(m).

Synthesis of 3: This compound was prepared similarly to **1**, with $CoCl_2 \cdot 6H_2O$ (0.48 g, 2 mmol) instead of $CdCl_2 \cdot 2.5H_2O$. Pink single crystals were obtained from the solution after 2 days. The yield was 55% (based on Co). Anal. Calcd. (Found) for $(H_3O^+)_3[\{Na(H_2O)_4\}\{Co(H_2O)_4\}_3(H_2W_{12}O_{42})] \cdot 24.5H_2O$: Na 0.59 (0.59); W 57.10 (57.23); Co 4.57 (4.60)%. IR (KBr pellet, cm^{-1}): 3348(vs), 1625(s), 939(s), 860(m), 713(m), 567(w), 495(m).

Synthesis of 4: This unexpected olive green crystals were obtained by using $NiCl_2 \cdot 6H_2O$ (0.47 g, 2 mmol) instead of $CdCl_2 \cdot 2.5H_2O$ under the similar conditions to **1**. The yield was 65% (based on Ni). Anal. Calcd. (Found) for $Na_4[NiW_6O_{24}H_6] \cdot 13H_2O$: Na 4.90 (5.12); W 58.75 (58.90); Ni 3.13 (3.27)%. IR (KBr pellet, cm^{-1}): 3436(vs), 1643(s), 898(m), 658(s), 459(m), 403(m).

2.3. Preparation of compound 3 modified CPE (3-CPE)

Compound **3** modified CPE (**3**-CPE) was fabricated as follows: 0.5 g graphite powder and 0.05 g compound **3** were mixed, and ground together by an agate mortar and pestle to achieve an even, dry mixture; to the mixture 0.5 mL paraffin oil was added and stirred with a glass rod; then the mixture was used to pack into 3 mm inner diameter glass tube, and the surface was pressed tightly onto weighing paper with a copper rod through the back. Electrical

contact was established with a copper rod through the back of the electrode.

2.4. X-ray crystallography

The reflection intensity data for **2** and **3** were collected on a Rigaku R-AXIS RAPID IP diffractometer with graphite monochromated Mo*K*α radiation at 293 K. The reflection intensities of **1** and **4** were collected on a SMART CCD diffractometer equipped with graphite monochromated Mo*K*α radiation at 208 K and room temperature, respectively, and an empirical absorption correction by SADABS was applied to the intensity data. All the structures were solved by direct methods and refined using the full-matrix least-squares method on F^2 with SHELXTL crystallographic software package. Anisotropic thermal parameters were refined for all non-hydrogen atoms, except for the water oxygen atoms. A summary of the crystallographic data and structure refinement for compounds **1**–**4** are given in Table 1. Further details of the crystal structure investigations of **1**–**4** may be obtained from the Fachinformationszentrum Karlsruhe, D-76344 Eggenstein-Leopoldshafen, Germany (E-mail: Crysdata@fiz-karlstruhe.de) on quoting the deposited numbers CSD-415830, CSD-415829, CSD-415828 and CSD-415847, respectively.

3. Results and discussion

3.1. Synthesis

Compound **1** was prepared from the mixture of Na_2WO_4, $CdCl_2$ and boric acid. It was an unexpected product during our attempts to synthesize borontungstate. When repeating the reaction without boric acid we cannot obtain compound **1**. It has been reported in the literature [12] that the $Al(NO_3)_3$ was added during synthesizing the $Na_{10}[H_2W_{12}O_{42}]$. Taking into account the characteristic comparability of identical group elements we think that the boric acid affects the formation of the $[H_2W_{12}O_{42}]^{10-}$ cluster although its role is not clear yet. Compound **3** can be obtained under the same reaction conditions. But attempts using $NiCl_2 \cdot 6H_2O$ failed to give crystals of the desired product in the whole range of pH (5–7.5), only the olive green crystals of $Na_4[NiW_6O_{24}H_6] \cdot 13H_2O$ have been obtained in high yield and purity. It is quite likely that the present synthesis conditions preferred the formation of Anderson-type polyanion $[NiW_6O_{24}H_6]^{4-}$ to paradodecatungstate clusters when Ni^{2+} is present. The report about Anderson-type polyoxotungstate is rare and the method mentioned here provides a convenient and effective route for the synthesis of $Na_4[NiW_6O_{24}H_6] \cdot xH_2O$. Considering that there is an obviously rare report of information on the Anderson-type polyoxotungstate with nickel as heteroatom, we give the crystal structure of $Na_4[NiW_6O_{24}H_6] \cdot 13H_2O$ (**4**) here.

Using the prefabricated precursor $Na_{10}[H_2W_{12}O_{42}] \cdot xH_2O$ [12] as starting reactant compound **2** that differs from **3** in structure can be obtained. The pH of the reaction mixtures seemed to be crucial because the solid is isolated only in a narrow pH region.

3.2. Crystal structure of compounds

The paratungstate-B unit observed in **1–3** is structurally identical to those reported previously, e.g. $K_6[Co(H_2O)_4]_2 \cdot$

Table 1
Crystal data and structure refinement for compounds **1**–**4**

	1	**2**	**3**	**4**
Empirical formula	$H_{70}Na_8CdO_{76}W_{12}$	$H_{74}Na_6Co_2O_{78}W_{12}$	$H_{92}NaCo_3O_{85.5}W_{12}$	$H_{32}Na_4NiW_6O_{37}$
Formula weight	3789.2	3784.06	3865.99	1878.10
Temperature/K	208(2)	293(2)	293(2)	293(2)
Space group	*P*−1	*P*−1	*P*−1	*P*−1
a/Å	12.766(6)	12.139(2)	12.293(3)	11.580(2)
b/Å	13.282(6)	12.418(3)	13.078(3)	12.458(3)
c/Å	13.282(6)	13.220(3)	14.903(3)	14.081(3)
α/°	64.55	68.21(3)	107.14(3)	108.22(3)
β/°	63.297(5)	71.17(3)	99.77(3)	113.73(3)
Γ/°	63.297(5)	71.34(3)	111.74(3)	92.84(3)
V/Å^3	1722.5(13)	1705.5(6)	2018.9(7)	1730.0(6)
Z	1	1	1	2
D_{calcd}/mg m^{-3}	3.585	3.685	3.104	3.543
μ/mm^{-1}	20.422	20.786	17.738	20.560
F(000)	1632	1706	1664	1624
Reflection collected	9541	5807	19287	11061
Independent reflections	6532	5807	9031	7706
R_1[a], wR_2[b] [$I > 2\sigma(I)$]	0.0388, 0.0980	0.0566, 0.1311	0.0513, 0.1068	0.0391, 0.1266
R_1, wR_2 (all data)	0.0466, 0.1010	0.0757, 0.1401	0.0747, 0.1158	0.0680, 0.1404
Absolute structure parameter		0.00		

[a] $R_1 = \Sigma(|F_o| - |F_c|)/\Sigma|F_o|$.
[b] $wR_2 = [\Sigma w(F_o^2 - F_c^2)^2/\Sigma w(F_o^2)^2]^{0.5}$.

$[H_2W_{12}O_{42}]\cdot 14H_2O$ [10], $Na_{10}[H_2W_{12}O_{42}]\cdot 20H_2O$ [12], $Mg_5[H_2W_{12}O_{42}]\cdot 38H_2O$ [13]. In compounds **1–3**, the $[H_2W_{12}O_{42}]^{10-}$ cluster acts as multidentate ligand coordinating to transition metal ions through terminal oxygen atoms (Fig. 1 left). The formation of different structures of these compounds depends on the connectivity of the transition metal cations. The coordination modes of the transition metal ions in compounds **1–3** are represent in Fig. 1 (right).

In compound **1**, the paratungstate $[H_2W_{12}O_{42}]^{10-}$ clusters act as tetradentate ligands coordinating to two cadmium(II) ions through the terminal oxygen atoms of four WO_6 belonging to the belt-type W_3O_{14} groups (Fig. 1A). The coordination site of the cadmium ions is a distorted octahedron formed by four oxygen atoms from two paratungstate groups and completed by two water molecules (Fig. 1a). So in the crystal of **1** the $[H_2W_{12}O_{42}]^{10-}$ clusters are interconnected through $[Cd(H_2O)_2]^{2+}$ bridging groups to form a infinite 1D chain, as shown in Fig. 2. The crystal structure of **2** contains a layer-like anionic polymer $[\{Co(H_2O)_3\}\{Co(H_2O)_4\}(H_2W_{12}O_{42})]_n^{6n-}$, formed by paradodecatungstate units linked together via six-coordinated cobalt bridges. There are two crystallographically unique cobalt centers with different coordination environments in **2**. Co(1) octahedra are formed by three oxygen atoms from two paratungstate cores, and completed by three H_2O molecules (Fig. 1b and Fig. 3). The Co(2) site is coordinated by two terminal oxygen atoms (which belong to two belt W_3O_{14} groups coming from two paradodecatungstate units) besides four H_2O molecules(Fig. 1c and Fig. 3), forming an distorted octahedron. Actually, for **2**, there is a disorder of repartition of Co(2) and Na(1) on the position according to the bond length (Table 2), and the best refinement result was obtained with occupation factors of about 0.5 and 0.5, respectively. In crystal of **2**, each cobalt ion links two $[H_2W_{12}O_{42}]^{10-}$ units, while each $[H_2W_{12}O_{42}]^{10-}$ block is surrounded by two $[Co(H_2O)_4]^{2+}$ and two $[Co(H_2O)_3]^{2+}$ bridging cations. Subsequently, a 2D sheet is formed parallel to the *ac* plane (Fig. 3). In compound **3**, the $[H_2W_{12}O_{42}]^{10-}$ anions are surrounded by six $[Co(H_2O)_4]^{2+}$ groups (symmetry equivalent included) (Fig. 1C). The Co(1), Co(2) and Co(3) cations are octahedral coordinated by four water molecules and two oxygen atoms from the two anions (Fig. 1c). In the crystal, the $[H_2W_{12}O_{42}]^{10-}$ anions are connected by bridging Co(1) and Co(2) into layers parallel to *bc* plane. These layers packing along the *a*-axis are further bound by Co(3) into a 3D structure with tunnels where disordered hydration water is located (Fig. S1). The structure of compound **3** can be approximately simplified as rhombus six-connected net for clarity: the clusters of building units are represented as pink nodes, and the bonds are represented as the edges, as shown in Fig. 4.

The anion $[NiW_6O_{24}H_6]^{4-}$ of compound **4** is presented in Fig. 5. This polyanion is typically the B-type Anderson structure [14,15] in which heteroatom Ni forms an closely regular octahedral complex of six OH groups with Ni–O

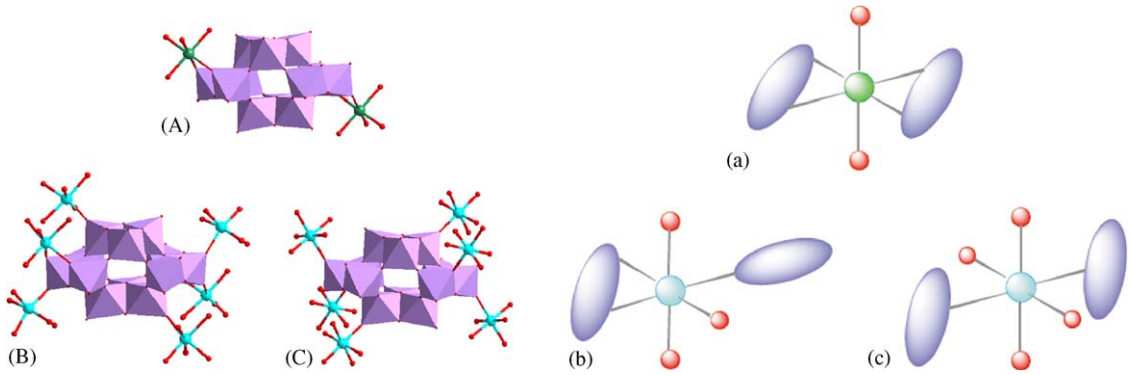

Fig. 1. Polyhedral and ball-and-stick representation (left) of: (A) $[\{Cd(H_2O)_2\}(H_2W_{12}O_{42})]^{8-}$ in compound **1**; (B) $[\{Co(H_2O)_3\}\{Co(H_2O)_4\}(H_2W_{12}O_{42})]^{6-}$ in compound **2**; (C) $[\{Co(H_2O)_3\}_3(H_2W_{12}O_{42})]^{4-}$ in compound **3** (WO_6 octahedra, purple; Co, cyanine; Cd, green; O, red); and illustration of the coordination modes of bridging transition metal sites (right): (a) cadmium–oxygen octahedron in **1** formed by four oxygen atoms from two $[H_2W_{12}O_{42}]^{10-}$ units and completed by two water molecules; (b) Co(1) octahedron in **2** formed by three oxygen atoms and three water molecules; (c) Co(2) octahedron in **2** and cobalt–oxygen octahedron in **3** formed by two oxygen atoms and four water molecules. ($[H_2W_{12}O_{42}]^{10-}$ cluster, purple ellipse; Cd, green circle; Co, cyanine circle and O of water molecules, red circle).

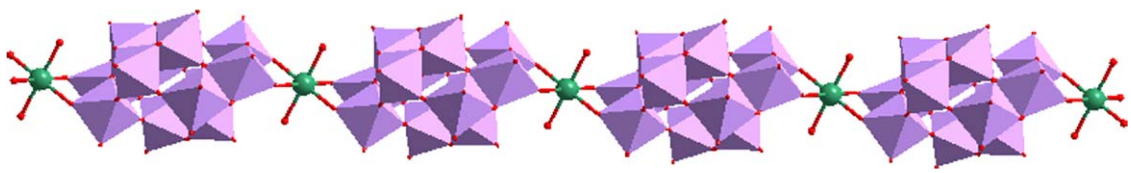

Fig. 2. Representation of the one-dimensional chain structure of compound **1**. (WO_6 octahedra, pruple; Cd, green; O, red).

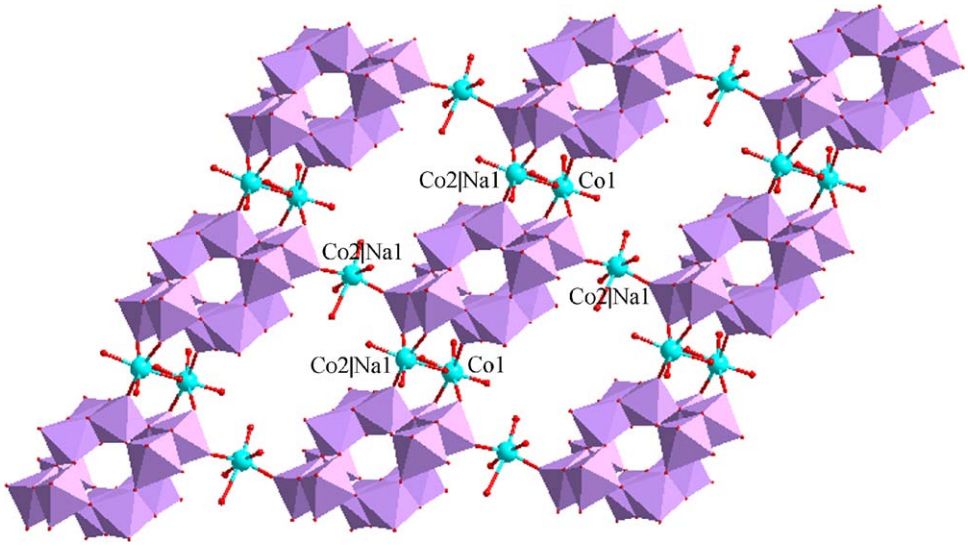

Fig. 3. A polyhedral and ball-and-stick representation of the layer structure of compound **2** (WO_6 octahedra, pruple; Co, cyanine; O, red).

Table 2
Selected bond length (Å) with standard deviations in parentheses of compounds **1**–**4**

	1 (M = Cd)	**2** (M = Co)	**3** (M = Co)	**4** (M = Ni)
M–O	2.253(8)–2.326(10)	Co(1)–O 1.89(5)–2.35(5) Co(2)|Na(1)–O1.95(5)–2.57(7)	2.045(8)–2.144(13)	1.992(12)–2.073(11)
Na–O	2.309(10)–2.594(12)	2.31(5)–2.66(7)	2.353(14)–2.581(9)	2.312(19)–2.610(2)
$W–O_t$[a]	1.703(7)–1.744(8)	1.566(4)–1.843(4)	1.735(10)–1.756(9)	1.707(11)–1.788(10)
$W–O_b(M)$[a]	1.779(8)–1.796(8)	1.619(5)–2.001(3)	1.742(10)–1.755(8)	
$W–O_b(W)$	1.808(8)–2.194(7)	1.512(3)–2.368(4)	1.742(10)–2.205(9)	1.924(11)–1.988(11)
$W–O_b(W, W)$	1.894(7)–2.283(8)	1.797(4)–2.407(3)	1.894(8)–2.289(8)	
$W–O_b(W, M)$				2.111(9)–2.305(11)

[a]The subscripts t and b refer to terminal and bringing oxo-groups.

distance about 2.04 Å, and six WO_6 octahedral edge-sharing units form a hexagon around the central $Ni(OH)_6$ octahedron. All of the metal atoms essentially lie in a common plane. The corresponding W–O distances can be divided into three groups: $W–O_t = 1.668(2)–1.815(2)$ Å, $W–O_b = 1.932(2)–1.981(9)$ Å, and $W–O_c = 2.112(2)–2.323(2)$ Å. In the crystal of **4**, the polyanions are held together by sodium to yield a planar sheet (Fig. S2).

3.3. Sorption/desorption of water molecules by compound *3*

Single-crystal X-ray diffraction studies reveal that compound **3** has tunnels occupied by a large number of guest water molecules. The solvent-accessible volume per unit cell is estimated to be 2018.9 $Å^3$ corresponding to 24.8% of the volume of the unit cell [16]. Thermal gravimetric (TG) analysis reveals that guest water molecules (11.4%) can be removed until 100 °C (Fig. S3). The as-synthesized pink crystalline solid was placed in a high vacuum oven at 65 °C for 5 h with a 11.1% weight loss to get the violet evacuated solid. When the dried sample was then exposed to the saturated water vapor at room temperature overnight, the water molecules were re-

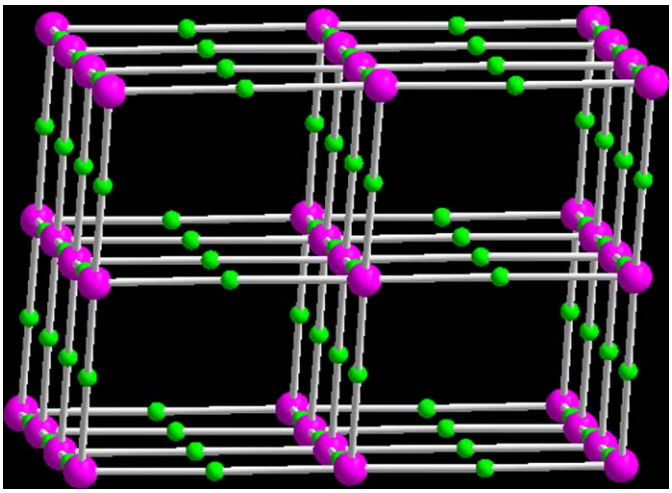

Fig. 4. Simplified schematic representation of the 3D network of **3**. The clusters of building units are replaced by pink nodes of the net, green represent Co, and all the water molecules are omitted for clarity.

adsorbed and the color recovered (Fig. S4). The stability of the 3D framework was further justified by the X-ray powder diffraction (XRPD) pattern (Fig. S5). The

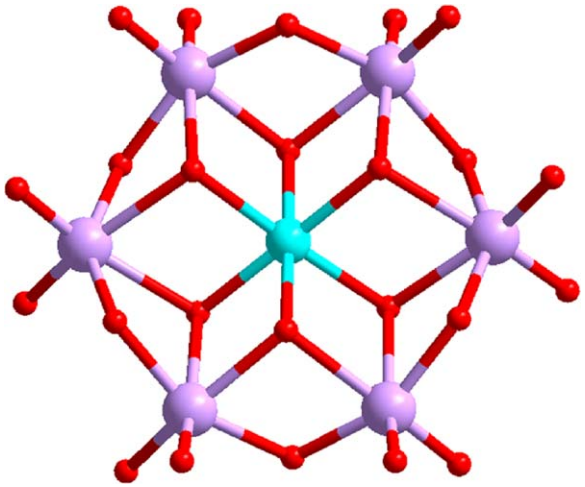

Fig. 5. View of the structure of the $[NiW_6O_{24}H_6]^{4-}$ in compound **4**. W, pruple; Ni, cyanine; O, red.

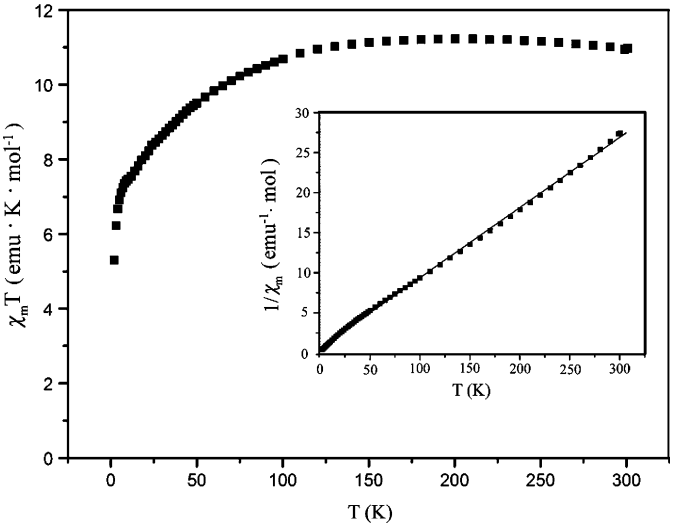

Fig. 6. Temperature dependence of magnetic susceptibility of compound **3** given by measurement of $1/\chi_m$ or $\chi_m T$ over a temperature range of 2–300 K.

evacuated solid remains crystalline order according to its XRPD pattern, albeit broadened and dissimilar relative to that of the original unevacuated solid. In the XRPD pattern of the re-hydrated solid, the peak positions and their intensities are essentially coincident to those observed for the as-synthesized solid, which demonstrates that the sample adsorbed water molecules and recovered the original structure with some loss of crystallinity.

3.4. Magnetic susceptibilities

The temperature dependence of the magnetic susceptibilities for compound **3** was measured from 2 to 300 K. Fig. 6 shows the magnetic behavior of polycrystalline samples of **3** in forms of $\chi_m T$ vs. T and $1/\chi_m$ vs. T plots. At 300 K, the effective magnetic moment (μ_{eff}) determined from the equation $\mu_{eff} = 2.828(\chi_m T)^{1/2}$ is 9.36 μ_B, which is much higher than that expected spin-only value (6.71 μ_B) for three magnetic isolated $S = 3/2$ Co(II) atoms probably due to the contribution of orbital angular momentum at high temperature [17]. Upon cooling from 300 K the value of $\chi_m T$ decreases continuously from 10.97 emu K mol^{-1} to a value of 5.30 emu K mol^{-1} at 2 K. The inverse susceptibility ($1/\chi_m$) plot as a function of temperature (T) is linear, closely following the Curie–Weiss law with $C = 11.42$ emu K mol^{-1}, $\theta = -7.11$ K. According to the crystal structure of **3**, it is clear that the magnetic superexchange must be very weak in this case. The decrease in the magnetic moment at low temperature upon cooling down must be mostly due to a strong influence of the zero-field splitting.

3.5. Electrochemical properties

Paratungstate belongs to the type III polyanion according to the category proposed by Pope [18], which contains not only WO_6 octahedra with single terminal oxygen but also the WO_6 octahedra with two *cis* terminal oxygen. So it is electrochemically active and can be reduced. The UV-vis spectra of all compounds were completely reproducible with respect to absorbance and wavelengths between pH 4 and 7 over a period of at least 24 h. The redox behaviors of parent compound $Na_{10}[H_2W_{12}O_{42}]$ and compounds **1–3** have been studied by cyclic voltammetry and described briefly.

The voltammetric pattern of $Na_{10}[H_2W_{12}O_{42}]$ in a sodium acetate buffer solution (0.4 mol L^{-1}, pH 5) shows a system of three pairs quasi-reversible waves, corresponding to tungsten redox process (Fig. 7a). Controlled potential electrolysis revealed that each of the three W reduction peaks corresponded to one-electron transfer process. Compounds **1–3** have the very similar pattern of voltammogram except for poor reversibility of the waves (Fig. 7b–d). The insufficient solubility of compounds **1–3** in aqueous solution prevented the NMR investigation. Without knowing anything about the integrity of the cluster in aqueous electrolytes made it is difficult to fully rationalize the voltammetric response. But these compounds are insoluble in common organic solvents; we can use them as modifiers to fabricate a bulk-modified carbon paste electrode (CPE) by the method proposed by Wang [19] to study the electrochemical behavior of solid in organic solvent. In this short account, only the result of **3**-CPE in 1,2-dichloroethane was discussed. The cyclic voltammetric behavior of **3**-CPE in 1,2-dichloroethane solution containing tetra-*n*-butylammonium perchlorate (TBA) (0.1 mol L^{-1}) as the supporting electrolyte shows three quasi-reversible redox peaks in the potential range from −600 to −1500 mV corresponding to the three one-electron processes of W. This observation is consistent with the results in aqueous solution, which indicated that the structure of anion $[H_2W_{12}O_{42}]^{10-}$ is preserved in solution after redissolution. Thus, the tungsten-oxo framework of the polyanion $[H_2W_{12}O_{42}]^{10-}$ could accept three electrons,

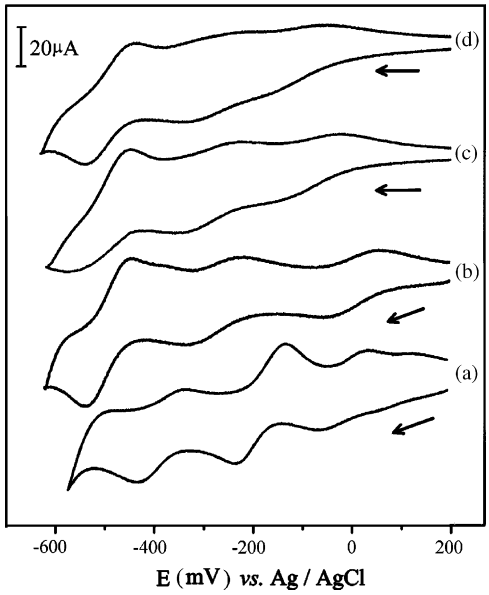

Fig. 7. Cyclic voltammetry at a glassy carbon working electrode of 2×10^{-4} mol L^{-1} compound solutions (0.4 mol L^{-1} sodium acetate buffer solution, pH 5, scan rate = 100 mV/s): (a) $Na_{10}[H_2W_{12}O_{42}]$; (b) **1**; (c) **2**; (d) **3**.

within the present experimental potential range. The redox potentials for W waves in dichloroethane were, in general, shifted towards more negative values than those in aqueous solution. This has been explained by considering Lewis interactions between the polyanions (bases) and the solvent molecules (acids) [20]. Except for the three waves corresponding to tungsten reduction, the oxidation processes at the metals Co^{II} can also be observed at **3**-CPE in positive potentials. Three oxidation peaks of identical intensity were detected at +497, 970 and 1487 mV, respectively. In the corresponding reduction scan, only two peaks at less positive potentials can be observed. This contrasts with the studies in aqueous solution, in which oxidation of metal was not detected by cyclic voltammetry. This observation maybe due to the insufficient solubility of **3** in aqueous solution or indicate that the oxidation $Co^{II}\rightarrow Co^{III}$ is more favorable in dichloroethane than in water. The number of electrons of each oxidation wave was estimated to one by comparison of the current of peaks with those of W waves. This observation indicated that the Co^{II} centers in compound **3** can be stepwise oxidized.

4. Conclusion

In summary, three new extended solids composed of transition metal cations and paradodecatungstate have been obtained and characterized. The different connection principle of the transition metals affects the dimensionalities of the frameworks. The synthesis methods described here provide new convenient and effective route for the synthesis of paratungstate cluster or $[NiW_6O_{24}H_6]^{4-}$ anion. The successful synthesis of compounds **1–3** indicates that paratungstate clusters are readily linked through secondary metal site into high-dimensional structures under conventional synthetic conditions and the $[H_2W_{12}O_{42}]^{10-}$ complex must be good candidates for designing new complex architectures with desired properties. The good redox activity and sorption properties of compound **3** are very advantageous to expand application of POM-based material in catalysis or guest-inclusion.

Acknowledgments

This work was supported by the National Science Foundation of China (Grant No. 20571014) and the Scientific Research Foundation for Returned Overseas Chinese Scholars, the Ministry of Education.

Appendix A. Supplementary data

Supplementary data associated with this article can be found in the online version at doi:10.1016/j.jssc.2006.03.048.

References

[1] (a) M.T. Pope, Heteropoly and Isopoly Oxometalates, vol. 1, Springer, New York, 1983;
(b) M.T. Pope, A. Müller, Polyoxometalate Chemistry from Topology via Self-Assembly to Applications, Kluwer Academic Publishers, Dordrecht, 2001;
(c) M.T. Pope, A. Müller, Angew. Chem. Int. Ed. Engl. 30 (1991) 34–48;
(d) J.T. Rhule, C.L. Hill, D.A. Judd, Chem. Rev. 98 (1998) 327–358;
(e) D.E. Katsoulis, Chem. Rev. 98 (1998) 359–388;
(f) N. Mizuno, M. Misono, Chem. Rev. 98 (1998) 199–218;
(g) J.B. Strong, G.P.A. Yap, R. Ostrander, L.M. Liable-Sands, A.L. Rheingold, R. Thouvenot, P. Gouzerh, E.A. Maatta, J. Am. Chem. Soc. 122 (2000) 639–649.
[2] H.T. Evans Jun., T.J.R. Weakley, G.B. Jameson, J. Chem. Soc. Dalton Trans. (1996) 2537–2541.
[3] A. Muller, M. Koop, P. Schiffels, H. Bögge, Chem. Commun. (1997) 1715–1717.
[4] G.S. Kim, H. Zeng, J.T. Rhule, I.A. Weinstock, C.L. Hill, Chem. Commun. (1999) 1651–1653.
[5] (a) A. Dolbecq, P. Mialane, L. Lisnard, J. Marrot, F. Sécheresse, Chem. Eur. J. 9 (2003) 2914–2920;
(b) S. Reinoso, P. Vitoria, L. Lezama, A. Luque, J.M. Gutiérrez-Zorrilla, Inorg. Chem. 42 (2003) 3709–3711;
(c) F. Bonhomme, J.P. Larentzos, T.M. Alam, E.J. Maginn, M. Nyman, Inorg. Chem. 44 (2005) 1774–1785;
(d) J.Y. Niu, M.L. Wei, J.P. Wang, D.B. Dang, Eur. J. Inorg. Chem. (2004) 160–170;
(e) P. Mialane, L. Lisnard, A. Mallard, J. Marrot, E. Antic-Fidancev, P. Aschehoug, D. Vivien, F. Sécheresse, Inorg. Chem. 42 (2003) 2102–2108.
[6] (a) J. Lü, E.H. Shen, Y.G. Li, D.R. Xiao, E.B. Wang, L. Xu, Cryst. Growth Des. 5 (2005) 65–67;
(b) C.M. Liu, D.Q. Zhang, D.B. Zhu, Cryst. Growth Des. 5 (2005) 1639–1642;
(c) Y. Lu, Y. Xu, E.B. Wang, J. Lu, C.W. Hu, L. Xu, Cryst. Growth Des. 5 (2005) 257–260;
(d) M. Liu, D.Q. Zhang, M. Xiong, D.B. Zhu, Chem. Commun. (2002) 1416–1417;

(e) D.J. Chesnut, D. Hagrman, P.J. Zapf, R.P. Hammond, R. Laduca, R.C. Haushalter, J. Zubieta, Coord. Chem. Rev. 192 (1999) 737–769;
(f) J.R.D. DeBord, R.C. Haushalter, L.M. Meyer, D.J. Rose, P.J. Zapf, J. Zubieta, Inorg. Chim. Acta 256 (1997) 165–168.
[7] (a) M.I. Khan, E. Yohannes, D. Powell, Chem. Commun. 0 (1999) 23–24;
(b) M.I. Khan, E. Yohannes, R. Doedens, J. Angew. Chem. Int. Ed. 38 (1999) 1292–1294;
(c) X.B. Cui, J.Q. Xu, H. Meng, S.T. Zheng, G.Y. Yang, Inorg. Chem. 43 (2004) 8005–8009.
[8] (a) K. Kalcber, Electroanalysis 2 (1990) 419;
(b) X.L. Wang, E.B. Wang, Y. Lan, C.W. Hu, Electroanalysis 14 (2002) 1116.
[9] H.T. Evans Jr., E. Prince, J. Am. Chem. Soc. 105 (1983) 4838–4839.
[10] C. Gimenez-Saiz, J.R. Galan-Mascaros, S. Triki, E. Coronado, L. Ouahab, Inorg. Chem. 34 (1995) 524–526.
[11] I. Loose, M. Bösing, R. Klein, B. Krebs, R.P. Schulz, B. Scharbert, Inorg. Chim. Acta 263 (1997) 99–108.
[12] H.T. Evans Jr., O.W. Rollins, Acta Crystallogr. Sect. B 32 (1976) 1565–1567.
[13] Y.H. Tsay, J.V. Silverton, Z. Kristallogr. 137 (1973) 256–259.
[14] G.A. Tsigdinos, Top. Curr. Chem. 76 (1978) 1–59.
[15] A. Perloff, Inorg. Chem. 9 (1970) 2228–2239.
[16] S.A.L. Platon, A Multipurpose Crystallographic Tool, Utrecht University, Utrecht, The Netherlands, 1998.
[17] O. Kahn, Molecular Magnetism, VCH, Weinheim, 1993.
[18] (a) M.T. Pope, Inorg. Chem. 11 (1972) 1973–1974;
(b) D.B. Brown, Mixed Valence Compounds, D. Reidel, Dordrecht, 1980, pp. 365–386.
[19] (a) X.L. Wang, Z.H. Kang, E.B. Wang, C.W. Hu, Chem. Lett. (2000) 1030;
(b) X.L. Wang, Z.H. Kang, E.B. Wang, C.W. Hu, Mater. Lett. 56 (2002) 393;
(c) X.L. Wang, H. Zhang, E.B. Wang, C.W. Hu, Mater. Lett. 58 (2004) 1661.
[20] B. Keita, D. Bouaziz, L. Nadjo, J. Electrochem. Soc. 135 (1988) 87–91.